Appl Phys B (2008) 92: 535–541
DOI 10.1007/s00340-008-3140-1

Applied Physics B
Lasers and Optics

Collinear broadband optical parametric generation in periodically poled lithium niobate crystals by group velocity matching

O. Prakash · H.-H. Lim · B.-J. Kim · K. Pandiyan · M. Cha · B.K. Rhee

Received: 12 February 2008 / Revised version: 9 June 2008 / Published online: 5 August 2008

Abstract Collinear broadband optical parametric generation (OPG) using periodically poled lithium niobate (PPLN) crystals were designed and experimentally demonstrated with the quasi-phase matching (QPM) periods of 21.5, 24.0, and 27.0 μm. The broad gain bandwidth was accomplished by choosing a specific set of the period and the pump wavelength that allows the group velocities of the signal and the idler to match close to the degeneracy point. OPG gain bandwidth and also the spectral region could be controlled by proper design of QPM period and pump wavelength. The total OPG gain bandwidth of 600, 900, and 1200 nm was observed for the PPLN devices with QPM periods of 21.5, 24.0, and 27.0 μm, respectively. We have also observed multiple color visible generation whenever the OPG spectrum was significantly broad. From the visible peaks of the three PPLN samples, it is found that broad gain bandwidth is crucial in the temperature-insensitive collinear simultaneous RGB generation from a single crystal.

PACS 42.65.Ky · 42.65.Yj · 42.65.Lm

1 Introduction

The broad quasi-phase matching (QPM) gain bandwidth in second-harmonic generation (SHG) or optical parametric amplification (OPA) is an essential requirement for the ultrafast laser applications [1, 2]. For frequency-doubling ultrafast pulses, for example, the SHG phase-matching bandwidth (or effective length of interaction) is limited by the group velocity mismatch between the fundamental and the second-harmonic pulses. Hence thin nonlinear crystals are necessary choice to broaden the bandwidth coming from the fact that it is inversely proportional to the interaction length in the first-order approximation. But shortening of the crystal length reduces the conversion efficiency significantly. Therefore, in order to broaden the phase-matching bandwidth without sacrificing the conversion efficiency too much, several methods have been reported in literature.

The first approach is to use the distributed (quasi) phase matching via aperiodic QPM gratings or multiple crystals. About 15 time enhancement in the bandwidth was reported for SHG by alternating the polarity of the QPM grating at certain positions along the interaction length [3]. Alford and Smith used multiple β-barium borate (BBO) crystals to phase-match different portions of the spectrum so that temporal walk-off is compensated in alternating segments, leading to bandwidth broadening [4]. The second approach is to utilize noncollinear interaction, where the broadband fundamental light is dispersed angularly so that each spectral component propagates at its phase-matching angle in critically phase matched crystals [5, 6].

Another efficient approach to broaden the SHG phase-matching bandwidth is the group-velocity matching (GVM) technique. In GVM SHG, the fundamental idea is to match the group velocities between the fundamental and the second harmonic in the desired spectral regions by using the material dispersion, while high conversion efficiency is achieved by QPM. The method of utilizing the GVM concept has advantages compared to the previous broadband methods because of its simplicity in the QPM design and fabrication

O. Prakash · H.-H. Lim · B.-J. Kim · K. Pandiyan · M. Cha (✉)
Department of Physics, Pusan National University,
Busan 609-735, Korea
e-mail: mcha@pnu.edu

B.K. Rhee
Department of Physics, Sogang University, CPO Box 1142,
Seoul 100-61, Korea

and collinear interaction, resulting in stable device operation and better output beam profiles. Arraf and de Sterke proposed broadband SHG in high-numerical aperture, step-index poled optical fibers by GVM method [7]. Hayata and Koshiba proposed femtosecond ultraviolet pulse generation by combined use of GVM and QPM SHG in BBO [8]. However, poling method for BBO has not yet been known, because it is not ferroelectric. The GVM SHG has been realized in MgO-doped, periodically poled lithium niobate (PPLN) crystal [9, 10].

The same GVM approach can be utilized in difference frequency generation (DFG) or OPA. Yanagawa et al. have obtained broadband DFG in around 2.0 μm region with a PPLN crystal for the application in IR spectroscopy for environmental gas detection [11]. Jeon et al. have reported efficient OPA of ∼100 nm broad signals in the communication band utilizing the GVM concept, where the QPM period and the pump wavelength were chosen to match the group velocities of the signal and the idler in the desired spectral region [2]. Lim et al. have recently demonstrated ultra-broadband optical parametric generation (OPG) and simultaneous RGB generation from PPLN using the GVM concept [12]. A CW-pumped ultra-broadband OPG has been reported by O'Donnell and U'Ren aiming at quantum optical applications with PPLN [13], where they indicated that ultra-broadening of the parametric bandwidth can be achieved by pumping at half the wavelength of the zero group-velocity dispersion (GVD) of the material [14]. Kuo et al. reported ultra-broad parametric gain band from 4.5 to 10.7 μm in an orientation-patterned GaAs crystal by choosing the degeneracy point (twice the pump wavelength) around (not exactly at) the point of zero-GVD, which is an equivalent concept to the GVM near the degeneracy point [15]. Similar experiment has been performed using a periodically poled $KTiPO_4$ crystal [16].

In this paper, we present the design and the experimental demonstration of an efficient collinear ultra-broad OPG gain bandwidth in PPLN crystals with different QPM periods. Both broadband OPG and collinear-cascaded white light generation are achieved by GVM near the degeneracy point. We show that the OPG gain bandwidth and the region of phase-matching wavelengths can be controlled by selecting a proper set of QPM period and pump wavelength. Effect of the temperature change in PPLN crystal on the OPG spectrum is also studied. The temperature dependence of collinear cascaded white light generation is investigated in detail according to the OPG spectrum change with temperature.

2 Theoretical consideration for ultra-broadband QPM OPG design

The QPM wave vector mismatch is given by $\Delta k_{\mathrm{QPM}} = \Delta k \pm 2\pi/\lambda$, where $\Delta k = k_p - k_s - k_i$ is the wave vector mismatch for DFG, k's denote the wave vectors for the pump (p), the signal (s), and the idler (i) waves, respectively, and Λ is the period of the QPM structure. Differentiating Δk_{QPM} with signal angular frequency ω_s for the fixed ω_p, we obtain

$$\frac{d\Delta k_{\mathrm{QPM}}}{d\omega_s} = \frac{d\Delta k}{d\omega_s} + \frac{d(2\pi/\Lambda)}{d\omega_s} \tag{1}$$

the first term

$$\begin{aligned}\frac{d\Delta k}{d\omega_s} &= \frac{d}{d\omega_s}(k_p - k_s - k_i) \\ &= -\frac{dk_s}{d\omega_s} - \frac{dk_i}{d\omega_s} = -\frac{dk_s}{d\omega_s} + \frac{dk_i}{d\omega_i} \\ &= v_{g,i}^{-1} - v_{g,s}^{-1}\end{aligned}$$

Here, $v_{g,i}$ and $v_{g,s}$ are the group velocities of the idler and the signal pulses, respectively. When the group velocities are matched ($v_{g,i} = v_{g,s}$) in the medium, $d\Delta k_{\mathrm{QPM}}/d\omega_s = 0$, then from (1) we can write

$$dl_c/d\lambda_s = 0 \tag{2}$$

where $l_c = \pi/\Delta k$ is the coherence length ($\Lambda/2$) and λ_s is the signal wavelength. This implies that the coherence length or the QPM period ($\Lambda = 2l_{c,}$) varies slowly over a wide wavelength range of the signal (and the idler).

Figure 1a shows the calculated group velocity of the light wave polarized along the optic axis of the lithium niobate, and the coherence length (or 1/2 QPM periods) for the three pump wavelengths of 822, 870, and 933 nm, respectively, based on the Sellmeier's formula for congruent lithium niobate reported by Jundt [17]. The zero-GVD point is located at 1918 nm (maximum of the group-velocity curve) as shown in the figure. When the degeneracy wavelength is slightly shorter than the zero-GVD point, one can expect signal fall in the shorter wavelength side of the maximum while the idler fall in the opposite side. Thus, their group velocities can be matched by choosing a proper pump wavelength. Since phase matching is not simultaneously satisfied with GVM in general, QPM is utilized to maximize the conversion efficiency (an exception is BiB_3O_6 crystal, which allows simultaneous GVM and phase matching for ultra-broadband OPG with pump at 800 nm [18]). From the figure one can clearly understand that, if one chooses a specific QPM period (horizontal line), which makes tangential contacts with the coherence length curve, a broad phase-matching OPG bandwidth is expected. Here, we have chosen local minima (degeneracy points) as tangential contacts,

although we could have chosen local maxima equivalently for the GVM. Thus the QPM periods required for the broad gain bandwidth at the pump wavelengths of 822, 870, and 933 nm, are 21.5, 24.0, and 27.0 μm, respectively (drawn by horizontal lines). Among these three cases, the coherence length curve with 933 nm pump seems to provide the broadest OPG band. This unique property occurs when the degeneracy point approaches the zero-GVD point as shown in Fig. 1a (the maximum of the group-velocity curve). In this case GVM conditions for the minima (degeneracy) and the maxima almost merge, which is the basis for the idea of pumping at the zero-GVD point [13, 14]. However, in order to obtain the maximum bandwidth, we see that the zero-GVD point (1918 nm) should be slightly detuned from the degeneracy point as mentioned in [14–16]. Slightly detuning the pump beam from the half of zero-GVD wavelength and choosing an appropriate QPM period to compensate the phase mismatch results in broader gain bandwidth [15].

The QPM wave vector mismatch $\Delta k_{\mathrm{QPM}} = \Delta k \pm 2\pi/\Lambda$ can be expanded around the signal (idler) central wavelength λ_0 as

$$\Delta k_{\mathrm{QPM}} = (\Delta k_{\mathrm{QPM}})_0 + \left[\frac{\partial(\Delta k_{\mathrm{QPM}})}{\partial\lambda}\right]_0 (\Delta\lambda) + \frac{1}{2}\left[\frac{\partial^2(\Delta k_{\mathrm{QPM}})}{\partial\lambda^2}\right]_0 (\Delta\lambda)^2 + \frac{1}{6}\left[\frac{\partial^3(\Delta k_{\mathrm{QPM}})}{\partial\lambda^3}\right]_0 (\Delta\lambda)^3 + \frac{1}{24}\left[\frac{\partial^4(\Delta k_{\mathrm{QPM}})}{\partial\lambda^4}\right]_0 (\Delta\lambda)^4 + \cdots \quad (3)$$

The first term, $(\Delta k_{\mathrm{QPM}})_0$, of (3) will be zero at the wavelength where QPM is satisfied. The terms having odd-order coefficients, i.e., second ($\frac{\partial(\Delta k_{\mathrm{QPM}})}{\partial\lambda}$) and fourth ($\frac{\partial^3(\Delta k_{\mathrm{QPM}})}{\partial\lambda^3}$) of the expansion, become zeroes when the central wavelengths of the signal and the idler match at the degeneracy point ($\lambda_{s0} = \lambda_{i0}$) [13]. Thus the bandwidth can be approximately calculated by the even order terms, i.e., third ($\frac{\partial^2(\Delta k_{\mathrm{QPM}})}{\partial\lambda^2}$) and fifth ($\frac{\partial^4(\Delta k_{\mathrm{QPM}})}{\partial\lambda^4}$) in (3). If the degeneracy point coincides with the zero-GVD wavelength, the contribution from the third term becomes zero and the bandwidth will be determined solely by the fifth term. In our experiment where the group velocities match near the degeneracy point and also away from the zero-GVD point, the bandwidth will be determined by the third, fourth, and the fifth terms of (3). The contribution from the first and second term will be zero due to QPM and GVM respectively.

The theoretically calculated OPG gain bandwidth under the low-gain limit is proportional to $\mathrm{sinc}^2(\Delta k_{\mathrm{QPM}}\ell/2)$, where ℓ is the length of the crystal. Figure 1b shows the normalized gain bandwidth for the three QPM periods of 27.0, 24.0, and 21.5 μm at the pump wavelengths of 933, 870, and 822 nm, respectively. The maximum OPG gain bandwidth for the QPM period of 27.0 μm was about 1300 nm for a 20 mm long PPLN. The gain bandwidth for QPM periods of 24.0 and 21.5 μm were 450 and 300 nm, respectively.

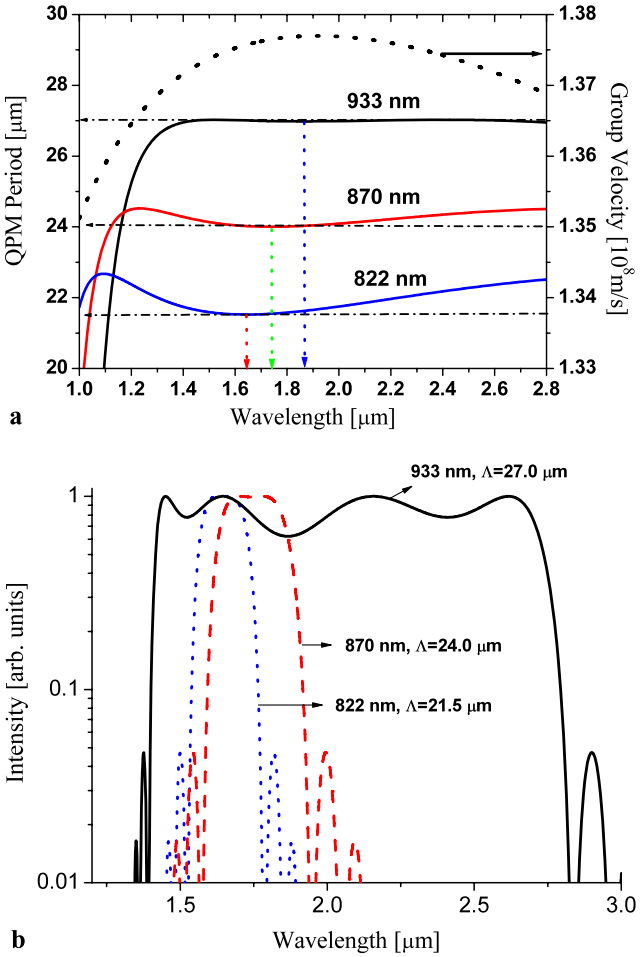

Fig. 1 (**a**) Group velocity (*dashed line*) and QPM period (*solid*) vs. signal, idler wavelength at the pump wavelengths of 933, 870, and 822 nm at 24°C for the PPLN crystal (vertical lines represent degeneracy points, horizontal lines represent selected QPM periods). (**b**) The OPG gain bandwidth under a small gain approximation for 10 mm long PPLN with QPM periods of 27.0, 24.0, and 21.5 μm at the pump wavelengths of 933 (*solid*), 870 (*dashed*), and 822 nm (*dotted*), respectively. Sample temperature was kept at 24°C for 27.0 and 24.0 μm and at 29°C for 21.5 μm for fine adjustment of the bandwidth

3 Experiment

The experimental setup for OPG is schematically described in Fig. 2. The pump light source was an OPG–OPA system using two β-BBO crystals, which were pumped by the third harmonic (355 nm) of the active–passive mode-locked Nd:YAG laser (Quantel YG901; pulse duration ∼35 ps, repetition rate ∼10 Hz). In this geometry, the first BBO gener-

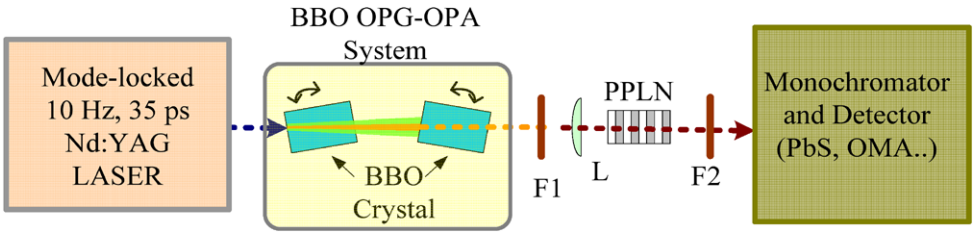

Fig. 2 Experimental setup of the OPG and simultaneous RGB generation

ated weak signal and idler by the proper orientation of the crystal, the central portion of the beam was further amplified by the second BBO crystal with the collinear 355 nm pump beam. The output of the OPG–OPA was tuned to the desired pump wavelengths for the OPG experiments. The pump beam was loosely focused into the PPLN crystal by the lens of the focal length of 5 cm. In the present experiment type-0 interaction is used, in which the pump, the signal, and the idler waves were polarized along the z-axis of the crystal. The PPLN crystal was placed in an oven with a temperature accuracy of ∼0.1°C. We used filters F-1 and F-2 for UV–Visible cut-off and band-pass from 1.2 to 2.5 μm, respectively. The OPG spectrum was measured with a monochromator (SPEX 1702) and a PbS detector (Thorlabs). The OPG spectrum was corrected to the spectral response of the detector only. While tuning the wavelength of the pump beam required for a specific QPM period of PPLN crystal to obtain the broadband OPG, we observed the change in the OPG spectrum.

The PPLN samples were fabricated by applying the standard electric field poling method to the 0.5 mm thick wafers of the congruent $LiNbO_3$ crystal (Yamaju Ceramics) with the liquid electrode at room temperature [19]. The PPLN crystal was z-cut and the z-axis of the crystal was perpendicular to the plane of the figure. The lengths of the PPLN samples along the crystalline x-axis (the light propagation axis of the pump beam) were 8.0 mm for the QPM periods of 21.5 and 24.0 μm and 20 mm for 27.0 μm, respectively.

4 Results and discussion

Figures 3a–c show the measured OPG spectrum at 24°C for the PPLN with QPM periods of 27.0, 24.0, and 21.5 μm at the pump wavelength of 933, 870, and 822 nm, respectively. We will designate the samples with QPM periods of 27.0, 24.0, and 21.5 μm as "A", "B", and "C", respectively, for the further discussion. For the sample A the OPG band starts from ∼1400 nm and ends at around 2600 nm as shown in Fig. 3a. A total bandwidth of about 1200 nm is observed for the sample A, and 900 nm (1400–2300 nm) and 600 nm (1400–2000 nm) for the samples B and C, respectively. Here, for the sample A the measured upper bound of the OPG band was limited by the transmission window of the band-pass filter. These results clearly show that the OPG spectrum of different bandwidth and spectral region is generated subject to the different QPM period.

For the sample A the generated OPG energy was 1.53 μJ at the pump energy of 17.3 μJ per pulse. With the same pump energy, the OPG output energy was 0.29 and 0.029 μJ for the samples B and C, respectively. The OPG power can be further improved by using a pump laser with better mode profile, and by an amplifier stage or double pass in the crystal. The double pass amplification in the PPLN crystal can be realized by using a dichroic mirror beyond the crystal, which selectively reflects the pump beam and transmits the OPG radiation. The OPG radiation and reflected pump beam are again reflected back to the crystal by two concave mirrors (reflectivity ∼100%) of suitable focal length reflecting OPG radiations and pump beam respectively. Note that there is a good agreement between the measured and the theoretically calculated OPG gain bandwidth as shown in Fig. 3a for the sample A. However, for the samples B and C, the experimentally measured OPG bandwidths were broader than the theoretically calculated ones (Figs. 3b and c). It is due to the larger fluctuation in duty-cycle for the samples B and C than in A. Broadening of SHG QPM bandwidth for the PPLN with large fluctuation in duty-cycle has been reported in literature [20, 21].

Although the pump wavelength and the QPM period are two crucial parameters to achieve an ultra-broad OPG bandwidth as shown in Fig. 1a, it also depends on the sample temperature through the Sellmeier's formula [17]. Therefore, we investigated the temperature dependence of the OPG bandwidth in the PPLN crystal. For this purpose, we used the sample A, which exhibited the broadest OPG gain bandwidth. Figure 4a shows the OPG spectra at three different temperatures of the sample A at the fixed pump wavelength of 933 nm and at the constant pump energy. Figure 4b shows theoretically calculated QPM periods versus signal, idler wavelength for three different temperatures at 933 nm pump beam. At 24°C, the coherence length curve $(\pi/\Delta k)$ makes nearly tangential contact with the horizontal QPM period line of $\Lambda = 27.0$ μm (the same graph in Fig. 1a). At higher temperature of 45°C, the coherence length curve does not meet the horizontal QPM period line and hence results in lower OPG intensity than that at 24°C. The OPG gain is also decreased at the central wavelength region which is more remote from the QPM line. The OPG gain spectrum is further

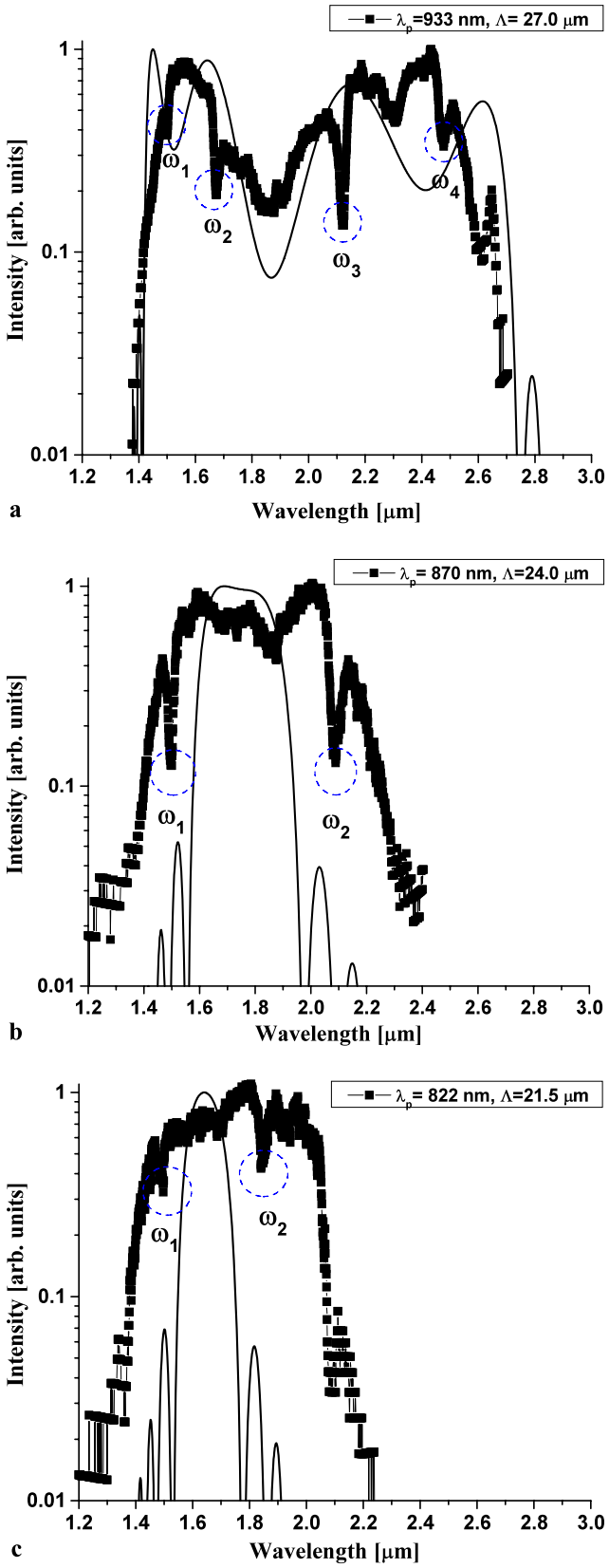

Fig. 3 OPG spectra at 24°C for the QPM period, pump wavelength of (**a**) 27.0, 933, (**b**) 24.0, 870, and (**c**) 21.5 μm, 822 nm, respectively. *Solid curves* are from the Sellmeier's formula

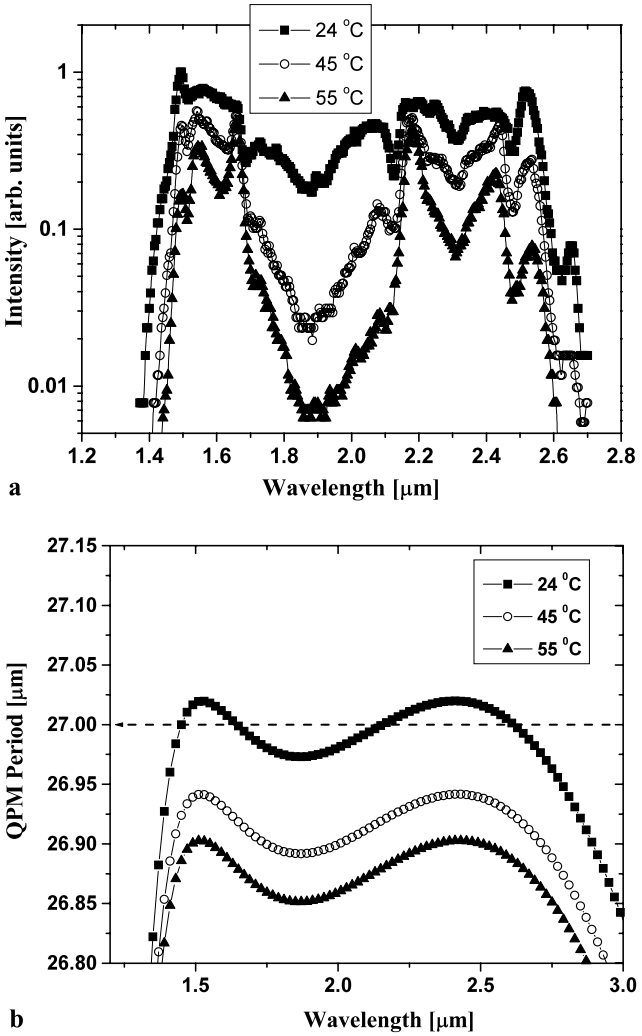

Fig. 4 (**a**) Experimental OPG spectra (for QPM period of 27.0 μm at pump 933 nm) at 24, 45, and 55°C, and (**b**) theoretically calculated QPM period vs. signal, idler wavelength

depleted and split into two as the temperature increases to 55°C.

We observed some visible lights collinearly with the pump, signal, and idler waves during the broadband OPG for all three samples. After recording and analyzing by a CCD spectrometer, it was revealed that the visible radiations consist of the three prime colors: red (R), green (G), and blue (B) [12]. The measured R, G, and B peaks for the three PPLN samples A, B, and C are shown in Figs. 5a–c. RGB peaks are clearly observed for A and B. We could observe only G and B peaks for the sample C. If we look at the OPG spectrum carefully, the sharp dips appear at certain wavelengths as indicated in Fig. 3. These dips are due to the high-order SFG between the pump beam and IR-OPG spectra as described in [12]. For the sample A the red peak is observed at 648 nm corresponding to the second-order QPM SFG between the dip at 2122 nm (ω_3) and the pump at 933 nm. The

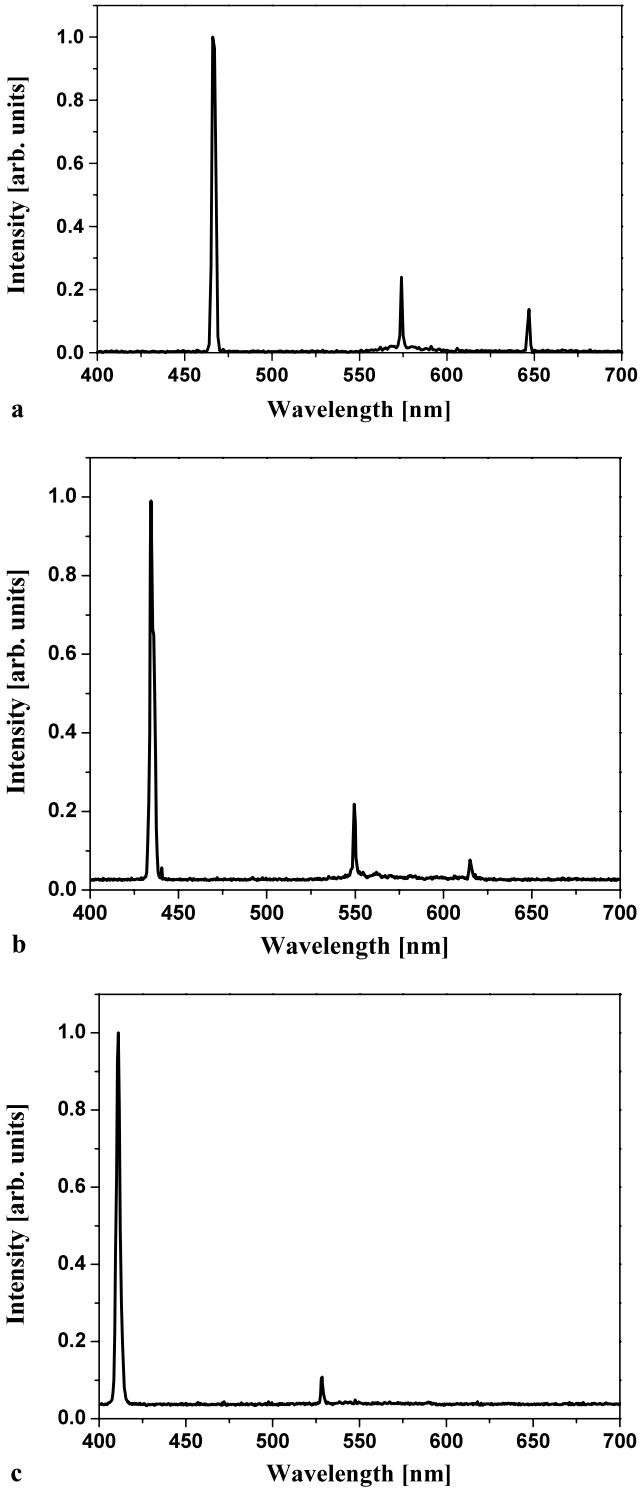

Fig. 5 RGB spectra for the PPLN crystals with the QPM period, pump wavelength of (**a**) 27.0, 933, (**b**) 24.0, 870, and (**c**) 21.5 μm, 822 nm, respectively

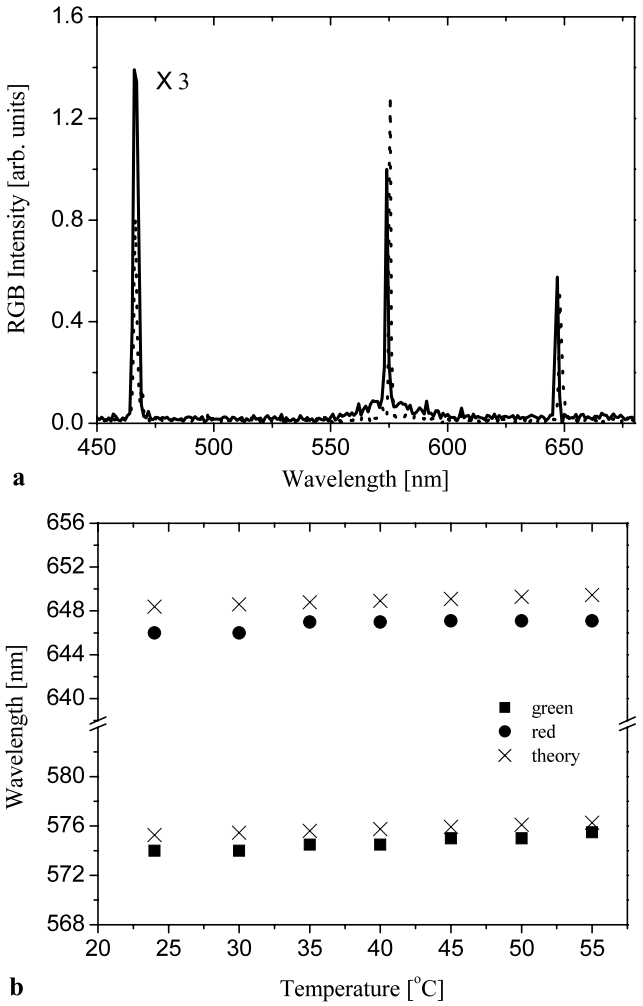

Fig. 6 (**a**) Variation of the RGB spectra with the temperature (24 (*solid*) and 55°C (*dotted*)) for the QPM period of 27.0 μm at the pump of 933 nm, and (**b**) wavelength shift in the G (*square*) and R (*circle*) peaks as a function of temperature along with the theoretically calculated values (*x*)

green peak at 575 nm is due to the third-order QPM SFG between the dip at 1498 nm (ω_1) and the pump. The dips at ω_2 and ω_4 are due to conjugate frequencies of ω_3 and ω_1, respectively. For the sample B, the dips at 1497 nm (ω_1) and 2068 nm (ω_2) occurred due to the generation of G and R peaks. In case of the sample C, the dip at 1483 nm (ω_1) is related to the generation of G light via SFG between pump and the corresponding depletion. The dip at 1850 nm (ω_2) is again conjugate to the dip at ω_1. For all the three QPM periods, the blue peak corresponds to the sixth-order QPM SHG of the pump itself. The even-order QPM processes are also possible due to the fact that the average duty-ratio of the actual periodic reversal is slightly different from 50%, and to the duty-cycle fluctuation of the QPM grating inherent to the fabrication process of PPLN [20]. We could not have observed R peak for the sample C because SFG phase-matching condition was not satisfied between the pump and the idler of the OPG. Thus, it is clear that the OPG gain bandwidth is crucial for the R and G generation.

It is seen that the OPG spectra change with the temperature of the PPLN crystal (Fig. 4a), therefore it is expected that the R, G, and B peaks will also be affected by the temperature change. The R, G, and B spectra at various temperatures were measured for the PPLN sample A at the fixed pump wavelength of 933 nm. Figure 6a shows the typical R, G, and B spectra at 24 and 55°C respectively. Here, it is clear that the change in the peak intensities and positions are not sensitive to a certain range of temperature change. Figure 6b also shows that the changes in the spectral locations of the R and G peaks are less than 1 nm for the temperature change from 24 to 55°C. This is consistent with the theoretically calculated shifts with the temperature using the Sellmeier's formula [17]. The small shift (<1 nm) in the position of R or G peaks is due to marginal change in the QPM SFG condition with temperature. Although the OPG spectrum changes significantly with the temperature in the middle part of the spectrum, the changes in the spectral components responsible for R and G generation are quite small. The robustness of RGB peaks against temperature change is one of the most important properties for practical applications.

5 Conclusion

We have designed and experimentally demonstrated the extremely broad OPG gain bandwidth using single PPLN crystal with three QPM periods of 27.0, 24.0, and 21.5 μm. The broadest OPG band was achieved by the group-velocity matching of the signal and the idler near the degeneracy point. The OPG bandwidth of more than 1200 nm was observed for the QPM period of 27.0 μm at the pump beam of 933 nm. The OPG bandwidth of 900 and 600 nm were obtained for the QPM periods of 24.0 and 21.5 μm, respectively. The broad OPG spectrum led to temperature insensitive collinear RGB light generation in a single PPLN period at a fixed pump wavelength.

Acknowledgements This work was partially supported by the Korea Research Foundation grant (KRF-2006-005-J02803) and by the Ministry of Commerce, Industry and Energy of Korea through the Industrial Technology Infrastructure Building program.

References

1. F. Rotermund, V. Petrov, F. Noack, V. Pesiskevicius, J. Hellstrom, F. Laurell, H. Hundertmark, P. Adel, C. Fallnich, Electron. Lett. **38**, 561 (2002)
2. O.Y. Jeon, M.J. Jin, H.H. Lim, B.J. Kim, M. Cha, Opt. Express **14**, 7210 (2006)
3. M.L. Bortz, M. Fujimura, M.M. Fejer, Electron. Lett. **30**, 34 (1994)
4. W.J. Alford, A.V. Smith, J. Opt. Soc. Am. B **18**, 515 (2001)
5. O.E. Martinez, IEEE J. Quantum Electron. **25**, 2464 (1989)
6. N. Fujioka, S. Ashihara, H. Ono, T. Shimura, K. Kuroda, J. Opt. Soc. Am. B **22**, 1283 (2005)
7. A. Arraf, C.M. de Sterke, IEEE J. Quantum Electron. **34**, 660 (1998)
8. K. Hayata, M. Koshiba, Appl. Phys. Lett. **62**, 2188 (1993)
9. N.E. Yu, J.H. Ro, M. Cha, S. Kurimura, T. Taira, Opt. Lett. **27**, 1046 (2002)
10. N.E. Yu, S. Kurimura, K. Kitamura, J.H. Ro, M. Cha, S. Ashihara, T. Shimura, K. Kuroda, T. Taira, Appl. Phys. Lett. **82**, 3388 (2003)
11. T. Yanagawa, H. Kanbara, O. Tadanaga, M. Osabe, H. Suzuki, J. Yumoto, Appl. Phys. Lett. **86**, 161106 (2005)
12. H.H. Lim, O. Prakash, B.J. Kim, K. Pandiyan, M. Cha, B.K. Rhee, Opt. Express **15**, 18294 (2007)
13. K.A. O'Donnell, A.B. U'Ren, Opt. Lett. **32**, 817 (2007)
14. A. Birmontas, A. Piskarskas, A. Stabinis, Sov. J. Quantum Electron. **13**, 1243 (1983)
15. P.S. Kuo, K.L. Vodopyanov, M.M. Fejer, D.M. Simanovskii, X. Yu, J.S. Harris, D. Bliss, D. Weyburne, Opt. Lett. **31**, 71 (2006)
16. M. Tiihonen, V. Pasiskevicius, A. Fragemann, C. Canalias, F. Laurell, Appl. Phys. B **85**, 73 (2006)
17. D.H. Jundt, Opt. Lett. **22**, 1553 (1997)
18. I. Nikolov, A. Gaydardzhiev, I. Buchvarov, P. Tzankov, F. Noack, V. Petrov, Opt. Lett. **32**, 3342 (2007)
19. L.E. Myers, G.D. Miller, R.C. Eckardt, M.M. Fejer, R.L. Byer, N.R. Bosenberg, Opt. Lett. **20**, 52 (1995)
20. M.M. Fejer, G.A. Magel, D.H. Jundt, R.L. Byer, IEEE J. Quantum. Electron. **28**, 2631 (1992)
21. D. Simeonov, S. Saltiel, in *Proceedings of Meetings in Physics at University of Sofia*, ed. by A. Proykova. vol. 5 (Heron, Sofia, 2004), pp. 26